Hydrology and Earth System Sciences

The topographic signature of Quaternary tectonic uplift in the Ardennes massif (Western Europe)

N. Sougnez and V. Vanacker

Université Catholique de Louvain, Earth and Life Institute, George Lemaître Centre for Earth and Climate Research, Louvain-la-Neuve, Belgium

Abstract. Geomorphic processes that produce and transport sediment, and incise river valleys are complex; and often difficult to quantify over longer timescales of 10^3 to 10^5 y. Morphometric indices that describe the topography of hill slopes, valleys and river channels have commonly been used to compare morphological characteristics between catchments and to relate them to hydrological and erosion processes. This study aims to analyze the link between tectonic uplift rates and landscape morphology based on slope and channel morphometric indexes. To achieve this objective, we selected 10 catchments of about 150 to 250 km² across the Ardennes Massif (a Palaeozoic massif of NW Europe, principally located in Belgium) that cover various tectonic domains with uplift rates ranging from about 0.06 to 0.20 mm yr^{-1} since mid-Pleistocene times. The morphometric analysis indicates that the slope and channel morphology of third-order catchments is not yet in topographic steady-state, and exhibits clear convexities in slope and river profiles. Our analysis indicates that the fluvial system is the main driver of topographic evolution and that the spatial pattern of uplift rates is reflected in the distribution of channel steepness and convexity. The spatial variation that we observe in slope and channel morphology between the 10 third-order catchments suggests that the response of the fluvial system was strongly diachronic, and that a transient signal of adjustment is migrating from the Meuse valley towards the Ardennian headwaters.

1 Introduction

There is great interest across a broad spectrum of geoscience disciplines in unravelling the role of tectonic activity in driving erosion processes and landscape evolution (Burbank et al., 1996; Maddy, 1997). Geomorphic processes that produce and transport sediment, and incise river valleys are complex; and often difficult to quantify over longer timescales of 10^3 to 10^5 yr. Morphometric indices that describe the topography of hill slopes, valleys and river channels have commonly been used to compare morphological characteristics between catchments and to quantify their potential hydrologic behaviour (Horton, 1932, 1945; Douvinet et al., 2007). The development and spreading of numerical tools (particularly geographical information systems) and the larger availability of multi-scale geographic datasets have facilitated the widespread use of morphometric parameters in geoscience studies. Nowadays, a whole range of catchment and river parameters exists, and Douvinet et al. (2005) highlighted 57 reference indexes.

More recently, those indices have been related to physical processes and landscape controls, such as stream-power models (Whipple and Tucker, 2002; Snyder et al., 2003; Whipple, 2004), stream sediment grain size variation (Surian, 2002; Rice and Church, 1998; Inoue, 1992; Petit et al., 2005), sea level and climate change (Bonnet and Crave, 2003; Roe et al., 2002; Whipple and al., 1999), and recent tectonic activity (Demoulin, 1998; Kirby and Whipple, 2001; Snyder et al., 2000). Most geomorphologic studies involving tectonic activity were concentrated in regions of high uplift rates and/or high denudation rates, such as the Himalayas (Burbank et al., 2003; Wobus et al., 2003; Lague and Davy, 2003), the Andes (Tibaldy and Leon, 2000; Kamp et al., 2005; Vanacker et al., 2007), and the Alps (Schneider et al., 2008; Musumeci et al., 2002; Norton et al., 2008; Brocard

Correspondence to: N. Sougnez
(nicolas.sougnez@uclouvain.be)

and van der Beek, 2006). The link between tectonics, erosion and morphology has rarely been analyzed in regions of low to moderate uplift rates (0.2–0.01 mm yr^{-1}; Tebbens et al., 2000; Demoulin, 1998; Lague et al., 2000).

The Ardennes Massif is an interesting field site for studying geomorphic processes. The area has been subject to differential tectonic movement: the northeastern part of the Massif is characterized by moderate uplift rates and seismic activity, whereas the western and southern parts are undergoing only slight epeirogenic upheaval (Pissart, 1974; Demoulin, 1995; Meyer and Stets, 1998; Garcia-Castellanos et al., 2000). Various authors have shown that in this context of low relief landscapes with low uplift rates, erosion increases with hillslope steepness (Ahnert, 1970) and local relief (Montgomery and Brandon, 2002). According to their observations, erosion rates can be linearly related to mean slope gradient or local relief. Following this hypothesis, spatial patterns of hillslope steepness can reflect spatial patterns in landscape-scale erosion rates in low relief areas and could be used to detect differential climatic or tectonic forcing. This also assumes that landscapes characterized by lower relief adjust quickly to changes in base level, and that hillslope processes are reflecting geomorphic response to disturbances.

The objective of this research is therefore to analyse if the present-day morphology can be used as an indicator of landscape response to tectonic activity. In these tectonic settings, we hypothesize that hillslope erosion is the main driver of topographic evolution. Therefore, we will test if the spatial pattern of uplift rates is reflected in the regional pattern of hillslope steepness and local relief. To achieve this objective, various morphometric indices have been derived from digital elevation data to capture the spatial variation in slope and channel morphology within the Ardennes Massif. We analysed possible correlation between the rock uplift pattern and slope and river channel indices; and performed a cluster analysis to explore spatial aggregation of geomorphic response to the NE-SW uplift gradient described by Demoulin and Hallot (2009).

2 Material and methods

2.1 Study area

The Ardennes Massif corresponds to the western part of the Rhenish shield which extends into Luxembourg and Germany (Fig. 1). The Cambrian massif consists of early Paleozoic metamorphic rocks, mostly phyllites and quartzites and is surrounded by Ordovician and early Devonian slates mainly to the south and east, and middle and late Devonian sandstones, shales and limestones in the north and west (Demoulin and Hallot, 2009). In this region, the North-Variscan fold-and-thrust belt has been superposed on structures from the old Caledonian orogeny. This results in a structurally
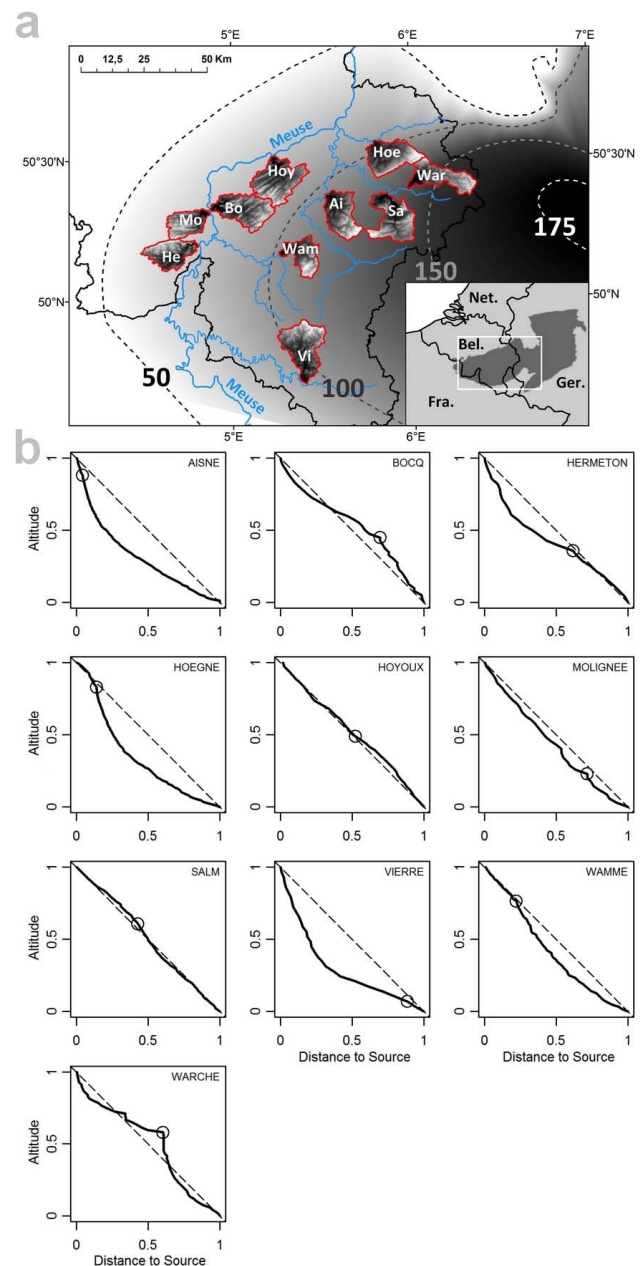

Fig. 1. (a) Location of the 10 catchments in the Ardennes-Rhenish Massif (inset map). The dotted lines correspond to the uplift isolines (values in meters) from Demoulin and Hallot (2009), and were derived from terrace sequences and planation surfaces. The names of the catchments are: Ai (Aisne), Bo (Bocq), He (Hermeton), Hoy (Hoyoux), Hoe (Hoegne), Mo (Molignée), Sa (Salm), Vi (Vierre), Wam (Wamme) and War (Warche). **(b)** Normalised longitudinal profiles of the 10 selected rivers with location of the main channel convexity (circle).

complex basement where longitudinal ENE-WSW folds and thrust faults are cut by NW-SE to NNW-SSE striking normal faults (Demoulin, 1998).

The Variscan folding was followed by an erosional phase (Vandycke, 2002). From the Permian until the Early Cretaceous, the Ardennes remained almost constantly below sea level. After the retreat of the upper Cretaceous sea, stepped planation surfaces developed. Their present-day elevations indicate that the region underwent rock uplift of about 450 m, and locally more than 500 m, since the Oligocene (Demoulin and Hallot, 2009). Strath terrace sequences of rivers draining the Ardennes Massif suggest that uplift rates accelerated during the Quaternary, with an increase of uplift rates at the Pliocene-Pleistocene transition and at the beginning of the middle Pleistocene to reach maximum uplift of 0.5 mm yr^{-1} in the Northeast Ardennes (Demoulin et al., 2009). Geomorphic data derived from terrace sequences of incised fluvial systems were commonly used to infer the spatial pattern of Quaternary uplift (van Balen et al., 2000; Garcia-Castellanos et al., 2000). Demoulin and Hallot (2009) recently proposed a modification of the shape and amount of the Quaternary uplift of the Ardennes based on a new interpretation of the incision data of intra-massif streams and additional geomorphological data. Lithospheric folding in response to intraplate compression in front of the alpine orogen (Cloetingh et al., 2005; Demoulin and Hallot, 2009) and upwelling of the Eifel mantle plume (and thermal thinning of the lithospheric mantle, Meyer and Stets, 1998; Garcia-Castellanos et al., 2000) are commonly cited as the two main causes of the Quaternary uplift of the Ardennes Massif. Nowadays, the Ardennes-Rhenish Massif is characterized by a moderate tectonic activity driven by intraplate motions (Camelbeeck, 2000; Cloetingh et al., 2005). The maximum uplift rate to which the Ardennes were subjected to was approximately 0.5 mm yr^{-1} (or 500 m per million years). Between 0.75 My and 0.4 My, the elevation of the north-eastern part has increased by 700 m.

We selected 10 catchments across the Ardennes Massif (Fig. 1a: Aisne, Bocq, Hermeton, Hoegne, Hoyoux, Molignée, Salm, Vierre, Wamme and Warche rivers) that have the same order of size (between 150 and 250 km^2) and for which consistent geological and elevation data are available. The limited amount of catchments studied can be explained by the following reasons. First, we limited our analyses to second or third-order rivers with minimum area of 150 km^2 to enable a valid comparison between the catchments and avoid scale related issues. Second, we restricted our analyses to catchments that are underlain by similar rock types (in our case, hard metamorphic rocks of the Palaeozoic era) to avoid as much as possible any influence of lithology. We also avoided areas where major fault systems have been identified. The geologic map of the Ardennes Massif is given in Fig. 2. Most catchments are third order catchments belonging to the Meuse River basin, one of the largest river basins in northern Europe with a catchment area of 36 000 km^2. Although the development of the Meuse river system started since the Eocene, the present day fluvial system was mainly established during the Pliocene period (Grimbérieux et al., 1995; Pissart, 1974; Pissart et al.,
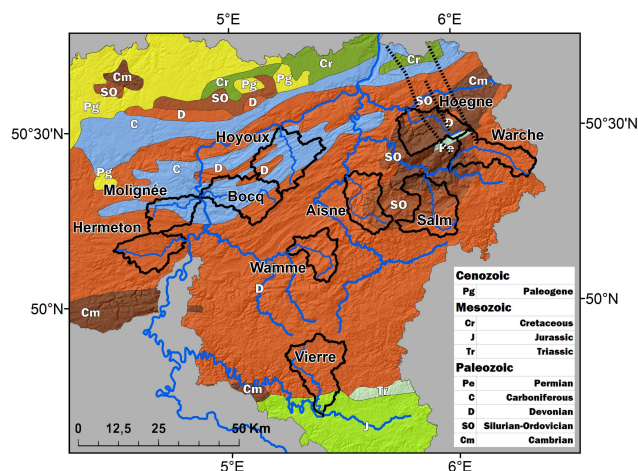

Fig. 2. Geologic map of the Ardennes Massif. The studied catchments are delimited in black, while the dotted lines on the NE represent the location of an active fault system (Hockaï Fault System).

1997). The selected catchments are covering a wide gradient of uplift rates ranging from about 0.06 to 0.20 mm yr^{-1} since mid-Pleistocene times according to the new map of post 0.73 Ma uplift by Demoulin and Hallot (2009). The catchments located in the north-eastern part of the Ardennes (Salm and Warche) have been subjected to the highest amount of uplift, whereas the catchments in the south-western part (Bocq, Hermeton, Hoyoux, Molignée) have been subjected to about half that amount.

In order to analyse links between tectonic uplift and river incision, we first analysed any possible influence of sea level change related to Quaternary climate change. In our study, we can consider that the effect of eustatic sea level change on the fluviomorphology of the third-order rivers is negligible. This assumption is based on several papers that demonstrate that the fall in sea level during the LGM caused incision only in the lower part of the river Meuse catchment (located in the Netherlands) (Törnqvist, 1998). The knickpoint created by the eustatic base level fall did not retreat further upstream than Maastricht (Veldkamp and van den Berg, 1993), and therefore did not reach the Ardennes Massif. The analyses of river terrace sequences in the Meuse confirm this (Juvigné and Renard, 1992; Van den Berg, 1996).

The presence of spatially uniform but temporally variable climatic conditions during the Quaternary affords a good opportunity to test the tectonic imprint on landscape evolution. Due to the relatively small size of the study area (latitudinal extent less than 100 km and longitudinal extent around 150 km), we hypothesize that all catchments have been subjected to rather similar climatic conditions. During the Quaternary glaciation cycles, the area was always located outside the permafrost area. According to the data of Schaller et al. (2004), the Quaternary climatic cycles only had minor impacts on the high erosion rates that are observed around

0.65 My ago. Nevertheless, it cannot be discarded that the observed Mid-Pleistocene increase in erosion rates resulted from the combination of increased tectonic activity during a period with strong increase in the magnitude of the glaciation cycles. Demoulin et al. (2009) suggested that the fluvial incision of the major streams in the Ardennes Massif can be regarded as the erosional response to the tectonic uplift, while weathering and erosion processes on the hillslopes are primarily controlled by changing climatic conditions. However, there is currently a paucity of quantitative data on rates of hill slope and river channel erosion to verify these different statements. It is possible that the non-steady character of the river morphology is partially related to climatically induced changes in sediment production and transport during the Quaternary, in conjunction to active tectonics. However, as we are focusing on *spatial* patterns in river and hillslope morphology in an area of *spatially relatively uniform climatic* conditions during the Quaternary, we assume that the temporal variability in climatic conditions is not affecting the robustness of our analyses.

2.2 Topographic and tectonic uplift data

Our study is based on the Digital Terrain Model (DTM) provided by the Belgian National Geographical Institute (IGN). We used the "DTM 1:10.000" product that is developed from photogrammetric derived points and structure-lines, airborne detail laserscanning and field point observations (IGN, 2008a). This product is a regular grid of 20 m resolution, and corresponds to the real ground surface. The use of a higher resolution DTM has also been tested: A LIDAR (Light Detection And Ranging) DEM data of 1 m resolution has been used in the Hoëgne catchment for the extraction of transversal and longitudinal profiles. An important amount of human induced artefacts have appeared in the profiles (roads, bridges, buildings, trees, etc.), and both automatic and manual removal could not completely remove these artefacts. These objects often form artificial barriers that block or force the flow calculations. Therefore, we decided to work with the DTM of 20 m resolution that is a good compromise between a coarse resolution (i.e. 50 m resolution) DTM that can skip some morphological features, and a very detailed elevation model (such as the LIDAR DEM) that can distort the calculations due to artefacts.

The dataset is reported to have RMS errors between 0.5 and 1.25 m horizontally and 1 and 1.6 m vertically (IGN, 2008b). The DTM provided by the IGN includes several artefacts (i.e. flat areas in the large valley plains, sinks inside narrow valleys, and staircases along the steepest hill slopes), and has to be processed before using it for hydrological applications. The initial levelling curves were reconstructed from the DTM data using the "Contour" function of ArcGis Spatial Analyst extension (the required input parameters to run this module are the digitalization scale, the altitude of the first known contour line, and the vertical equidis-

tance between the initial curves). Then we re-interpolated the contour lines using the "Topo to Raster" ArcGis function to obtain a continuously varying 3-D surface of 20 m resolution. In this module, additional information (constraints, hill top point features and linear ridges) was used to optimize the interpolation and produce a more accurate DTM. The natural sinks that remain in the DTM were filled using the Hydro-Tools ArcGis extension (Filling-Sink tool) written by Schäuble (2000). We also applied the sink identification and filling method provided by Wang and Liu (2006), and compared the results. In our study, less than 2% of the total pixels were different between the interpolated surfaces and differences were significantly (95%) lower than 0.5 m. According to recent work on DEM pre-processing (i.e. Santini et al., 2009; Nardi et al., 2008 and Grimaldi et al., 2007), the use of advanced flat-area treatment and pre-processing tools for channel network extraction significantly improves the DEM accuracy. These algorithms are particularly interesting for flat areas. In our dataset, flat areas have been detected only in large valley plains of first to second order rivers (i.e. Meuse river). As <1% of the area of our third order catchments is flat, we used traditional techniques that are available in standard GIS software for channel network extraction. The channel network was therefore identified using the "Flow Accumulation" ArcGis function on the corrected DTM. This function uses the Deterministic-8 flow direction approach and creates a linear flow raster. A threshold has then been set on the Flow Accumulation raster independently for each stream. The river headwater location was determined from Google Earth georeferenced images and orthorectified aerial photographs. To avoid parallel flux lines, the "Stream to Feature" ArcGis module was used to obtain stream shapefiles that are closer to the real hydrological network according to Tarboton et al. (1991). To extract the longitudinal profiles, we used the intersections of the contour lines with the flow line of the river (so the longitudinal profile has been exempted by flat areas that eventually may occur in some large valley plains). We used the D8 algorithm to derive drainage area. The transversal profiles were directly derived from the DTM.

The spatial pattern of tectonic uplift (MU, in m, see Table 1) was derived from the uplift isolines presented by Demoulin and Hallot (2009). In this paper, the uplift amounts correspond to the uplift that follows 0.73 My. Those amounts of uplift (given in m) can easily be converted into uplift rates (m My^{-1}) by dividing the uplift amplitude by 0.73. A mean uplift value was then calculated for each catchment. The uplift isolines presented in the paper of Demoulin and Hallot (2009) are based on the stratigraphy of the river terraces of the Meuse and Rhine-Mosel rivers, and the uplift pattern has been confirmed by geomorphic and more recently by seismic tomography studies. Demoulin and Hallot (2009) reconstructed past geomorphic features (Tertiary planation surfaces) to corroborate roughly the history of the uplift. The tertiary landscape of the Ardennes and Rhenish

Shield was composed of sub-horizontal planation surfaces that have been formed in tropical conditions at low altitudes. The fact that these planation surfaces were almost horizontal during Tertiary era makes them an ideal marker for subsequent deformation (i.e. the Quaternary uplift). Recent papers have used seismic tomography techniques to create a thermal model of the European lithosphere (Tesauro et al., 2009 based on the observations of Ritter et al., 2001). We may interpret their results in terms of thinning of the lithospheric mantle in this region, and the map of the temperature variation at 60km depth shows an important gradient in our area of interest, varying from 1100 °C on the Eastern Ardennes to 800 °C on the western part. These results from numerical models are conforming to the uplift pattern that was proposed by Demoulin and Hallot (2009) based on terrace stratigraphy and planation surfaces.

2.3 Morphometric indexes

First, standard morphometric indices that capture the overall slope morphology were derived. These morphometric indices (index of Gravelius, Horton and Schumm, Eqs. 1, 2 and 3) were extracted to compare the overall 2-D geometrical shape between the catchments (Table 1). These indices use a combination of shape metrics (perimeter, area and length) to describe quantitatively the geometry the watersheds. We assume that catchments that are subject to high rates of tectonic uplift would be prone to have an elongated shape, and that catchments located in tectonically quiet regions would rather be characterized by a dendritic river network and a round catchment shape (Burbank and Anderson, 2000). The indices of Schumm (Sc, in $m\,m^{-1}$) and Horton (Ho, in $m\,m^{-1}$) have the advantage of not being scale-dependent, which is not the case for the index of Gravelius (Gr, in $m\,m^{-1}$) that proved to be highly raster resolution dependent (Senadeera et al., 2004).

$$Gr = \frac{P}{2\sqrt{\pi A}} \tag{1}$$

$$Ho = \frac{A}{L^2} \tag{2}$$

$$Sc = \frac{2\sqrt{\frac{A}{\pi}}}{L} \tag{3}$$

with P, the perimeter of the catchment (m), A the catchment surface (m^2) and L, the maximum extent of the catchment (m)

To get an insight in the spatial distribution of the slope morphology within the catchments, slope and local relief maps were derived from the DTM. The Local Relief index was used to quantify the local variation in altitude within the catchments. This index can directly be used to assess catchment-wide hillslope steepness values. Catchments with a higher Local Relief Index are assumed to be subject to a

greater tectonic influence than catchments presenting a low LR value. The slope raster has been directly obtained using the "Slope" ArcGis function, while the Local Relief maps were calculated in the Neighbourhood Statistics module of the ArcGis software. The local relief map has been generated using a 5×5 moving window (also called roving-window technique, Grohmann and Riccomini, 2009) which calculates in the central cell, the range between the min and max values observed in the window. The local relief describes the complexity of the landscape at a larger scale than the original data and can reflect the degree of incision (i.e. a river, Montgomery and Brandon, 2002). A local relief index (LRel, in m) was computed on the basis of the local relief map, and consists of the median value of all local relief values within the catchment. The choice of the median can be explained by the fact that this metric is less sensitive to extreme values than the arithmetic mean.

$$LRel_i = \frac{\sum_i (Z_{max} - Z_{min})}{n} \tag{4}$$

with Z_{max} and Z_{min}, the maximum and minimum altitude (m) pixel value observed in the roving-window, and n, the number of pixels in the catchment.

Second, we focused on the river channel morphology. For each catchment we extracted the river longitudinal profiles and several transversal profiles based on the original levelling curves. The transversal topographic profiles were extracted perpendicularly to the river channel at sections that are not affected by local morphological changes related to river confluences. The location of the transversal profiles was selected manually along the river channel, thereby avoiding areas of confluence with the main tributaries where we can detect a decrease of proximal slopes. For each river, more than 20 transversal profiles were extracted. The eight most representative transversal profiles with minimal effect of anthropogenic artefacts (such as roads, reservoirs, or villages) were then selected for further analysis. Stream proximal slope (S_i, in %) and curvature (C_i, in m^{-1}) were calculated using the following equations:

$$S_i = \frac{(y_{i-1}) - (y_{i+1})}{(x_{i-1}) - (x_{i+1})} \cdot 100 \tag{5}$$

$$C_i = \frac{\left(\frac{(y_{i+2}) - (y_i)}{(x_{i+2}) - (x_i)}\right) - \left(\frac{(y_i) - (y_{i-2})}{(x_i) - (x_{i-2})}\right)}{(x_{i+2}) - (x_{i-2})} \tag{6}$$

with x_i = upstream distance (m), and y_i = altitude (m) at point i.

Slope-Area diagrams were constructed to identify knick zones in the longitudinal profiles. Knickpoints can be created by different processes like lithological contrasts along the channel, heterogeneous sedimentary load, base level drops following sea level changes, and tectonic activity that can increase the relief locally or even regionally (Snyder et al.,

2000; Whipple, 2004). Only the knickpoints that are not related to clear lithological contrasts according to the 1/50 000 geological maps of the area were selected in our analyses.

The slope-area diagrams of the different river basins were constructed by combining the flow accumulation raster with the slope raster of the river sections. For each river, we divided the streamline into several segments that correspond to the part of streamline included between two following contour lines in the topographic dataset. The drainage area (x axis) was calculated at every intersection of the streamline with the contour lines using the flow accumulation raster, and the slope (y axis) was calculated by dividing the interval of the contour lines (i.e. one meter) by the flow path distance of each river segment. The relations between A and S are typically following a negative power function, and are commonly represented on a log-log graph (Whipple, 2004). For each river, we fitted an inverse power law equation (so-called Flint law) between the drainage area (A, in m^2) and the river channel gradient (S, in m m^{-1}):

$$S = k_s A^{-\theta} \tag{7}$$

The empirically derived parameters k_s and θ can be used as indicators of respectively the steepness and concavity of the river longitudinal profile (Flint, 1974; Hack, 1973; Whipple, 2004). Under steady-state conditions, a balance is expected to exist between local channel steepness and the upstream drainage area. The overall channel steepness k_s has frequently been used as an indicator of the relationship between net uplift and net erosion (Howard, 1994; Whipple and Tucker, 1999). However, it should be noted that in areas with geo-structural heterogeneity, local oscillations of base level and/or climatic conditions, the tectonic imprint on river channel morphology might be far more difficult to discern.

A comparison of the observed Slope-Area relationships for the 10 rivers in the Ardennes Massif allows us to compare the channel morphology of rivers draining highly different tectonic regimes. As the empirically derived value of the steepness index (k_s) is dependent on the profile concavity, we normalised the steepness values (k_{sn}) to a reference concavity, θ_r, of 0.45 following Snyder et al. (2000) and Kirby et al. (2000). The normalised steepness values, k_{sn}, can then be used to compare the steepness between different river systems; with larger values of k_{sn} representing steeper rivers.

In addition to these parameters, we derived an area-normalized stream concavity index (SCI) of each river channel as defined by Demoulin (1998) and Zaprowski et al. (2005). The SCI is a measure of the surface between the normalised longitudinal profile and a straight line joining the source and the outlet of the catchment (Eq. 8):

$$SCI_i = 1 - \sum_{i=0}^{1} ((x_i - x_{i+1})(y_i + y_{i+1})) \tag{8}$$

with $x_i =$ upstream distance (m), and $y_i =$ altitude (m) at point i. If the stream profile is above the reference line, the area between the two is considered negative. A river profile with positive SCI value will be considered as concave up, and a negative value is an indicator of a convex up river profile (Zaprowski et al., 2005). We slightly modified the initial formulation of the index so that the values range between ± 1, with an equilibrium concave up longitudinal profile having a SCI of about 0.5. Convexities in the river profiles often indicate disequilibrium along the river stream course that can be related to unsteady tectonic or climatic conditions.

We analysed then the hypsometry of the catchments to get a measure of the overall slope and channel morphology. The hypsometric integral, HI, was calculated as follows:

$$HI_i = \sum_{i=0}^{1} \frac{1}{2} (y_{i+1} + y_i)(x_{i+1} - x_i) \tag{9}$$

where $x_i =$ upstream distance (m), and $y_i =$ altitude (m). The hypsometric integral is a measure of the distribution of landmass volume above a basal reference plane, and can be interpreted in terms of relative landform age (Strahler, 1952). Differences in the shape of the hypsometric curve have been related to differences in erosive and tectonic processes (Weissel et al., 1994), and the value of the hypsometric integral has been understand as an indicator of the degree of disequilibrium in the balance between erosive and tectonic forces for a particular landform (Luo, 1998). When comparing the morphology of catchments, the catchment with the highest value of HI has the largest amount of landmass above the outlet, and this can be interpreted in terms of lower erosion or higher tectonic activity. As our catchments have comparable size (150 to 250 km^2), the scale-dependency of the hypsometric integral should not directly affect our results (Willgoose and Hancock, 1998).

In addition to the morphometric indices that are described above, we calculated two parameters that are linked to the position of the knick zone: Ach and Rch, respectively the absolute (i.e. height above sea level, m) and relative (i.e. height above the altitude of the catchment outlet, m) height of the top of the main stream convexity. Knickpoints were identified based on the river longitudinal profiles and the slope-area diagrams, and they correspond to the river section with the greatest curvature value. We then carefully analysed any possible influence of lithology or fault systems. In some catchments, knickpoints have developed where lithological contrasts are present. They are visible in the longitudinal profiles, and are typically of minor vertical amplitude (between 5 to 10 m) and spatially limited to a narrow zone. They can be differentiated from the tectonic knickpoints that have a much larger vertical extension and extend over several hundred meters.

2.4 Statistical analyses

In order to test the possible link between the tectonic activity and the catchment morphology, we applied correlation

Table 1. Morphometric indices: S = surface; P = perimeter; MU = mean uplift (according to Demoulin and Hallot, 2009); Ach and Rch = the absolute and relative height of the convexities (in meters); LRel = the median of the local relief in a 100 m range window; ho = the altitude of outlet; Gr, Ho and Sc = the classical morphometric indices (Gravelius, Horton and Shumm); θ and Ksn = convexity and normalised steepness indices (Flint law); HI = the hypsometry integral; and SCI = the stream convexity index.

Rivers	S	P	MU	Ach	Rch	LRel	ho	Gr	Ho	Sc	θ	Ksn	HI	SCI
	(km^2)	(km)	(m)	(m a.s.l.)	(m)	(m)	(m a.s.l.)	(m m^{-1})	(m m^{-1})	(m m^{-1})	(–)	(–)	(–)	(–)
Aisne	190.6	71.0	115	450	315	10.85	135	1.439	0.441	0.750	0.478	44.45	0.251	0.379
Bocq	235.4	89.0	84	195	100	6.62	95	1.624	0.341	0.659	0.478	38.50	0.523	−0.055
Hermeton	169.3	69.6	69	150	50	4.72	100	1.498	0.316	0.635	0.323	13.25	0.442	0.165
Hoegne	208.6	75.1	110	510	375	7.83	135	1.456	0.356	0.673	0.552	72.19	0.221	0.316
Hoyoux	255.7	94.6	86	200	125	5.20	75	1.656	0.570	0.852	0.017	26.15	0.481	0.002
Molignée	139.3	58.5	70	150	60	6.01	90	1.388	0.384	0.699	0.138	18.77	0.376	0.145
Salm	238.0	90.3	133	460	210	7.12	250	1.640	0.423	0.734	0.052	24.39	0.422	−0.002
Vierre	259.1	89.2	103	330	10	6.27	320	1.551	0.374	0.690	0.519	13.62	0.263	0.408
Wamme	140.2	68.8	109	430	245	7.83	185	1.627	0.440	0.748	0.196	38.93	0.308	0.178
Warche	191.2	94.7	146	522.5	222.5	6.30	300	1.918	0.245	0.558	0.513	95.51	0.484	0.011

and spatial clustering techniques. We performed a correlation analysis to evaluate possible relation between the morphometric parameters and the MU of the catchments. In order to classify the catchments "objectively" according to their different properties, a multivariate statistical classification method has been chosen. This technique was applied to identify the indices that are most likely to represent the observed spatial variability in slope and channel morphology. We used the Ward's unsupervised classification procedure on the normalized morphometric indices to identify the optimal number of profile types, and a K-means clustering method to recognize the weight of each parameter in the classification process (Lu et al., 2004).

3 Results

Our morphometric analysis indicates that large differences exist in slope and channel morphology between the selected catchments (Fig. 1, Table 1). There exists also morphological heterogeneity within most of the catchments (between the upstream section and downstream the knickzones, see discussion). The catchments in the western and southern part of the Ardennes Massif are more prone to have relatively smooth river and channel profiles. In the northeastern part of the Ardennes Massif, we observed various catchments with irregular non-equilibrium slope and channel profiles, and the presence of clear knick zones. However, this concept cannot be generalized; and there are also several rivers that present typical concave up profiles (in equilibrium state, with SCI ~0.5, like the Vierre in our dataset).

We observe that the elevation of the shoulder (upper part) of the river channel convexity is related to the mean uplift: catchments that are located in regions with higher uplift rates generally have knick zones at higher altitude (Fig. 3a). This relationship may seem self-evident, as the mean elevation of the catchment is expected to be directly related to the total amount of uplift. However, this observation also implies that knickpoints do not dissipate rapidly in low relief terrain with low to moderate uplift rates.

We observed also some correlation between the mean uplift of the catchments and the stream concavity index: rivers with concave up longitudinal profiles are generally located in zones with low uplift rates, while river with clear convexities in their long profile are more concentrated in the region with higher rates of tectonic uplift (Fig. 3b). However, not all convex reaches are located in zones of high uplift rates (two circles in Fig. 3b). This might be related to the presence of weaker lithology (presence of carboniferous rocks in the majority of the streams courses – C class in Fig. 2), but also to local tectonic activity. Indeed, the presence of a local centre of subsidence in the Namur area is under study (anomalies in the river terraces can be observed in this region according to Pissart and Lambot, 1989; Demoulin, 1998) and is not represented in the uplift data of Demoulin and Hallot (2009).

A K-means cluster analysis was performed to identify groups of catchments with similar patterns of slope and channel morphology. The Ward's hierarchical classification method was used. A reduced number of variables was selected to avoid auto-correlation in the analysis: Rch, Ho, k_{sn}, HI and SCI. Those parameters are representative of the various aspects of the slope and channel morphology: Rch for the river knickpoint position, Ho as a measure of the shape of the catchment, k_{sn} as an index for the general slope (steepness) of the river channel, HI as a measure of the catchment relief and SCI as an index of the general shape of the river longitudinal profile. Table 2 shows the main characteristics of the three groups that were recognized by the statistical procedure, and gives the mean value and the standard deviation associated to each cluster. Given the small number of observations, these numbers should be regarded with caution.

Table 2. Clusters characteristics (values of mean and standard deviation of the parameters).

Cluster	Rivers		Rch	Ho	Ksn	HI	SCI
1	Aisne, Wamme, Hoegne	Mean	311.7	0.412	51.9	0.260	0.291
		StD	65.06	0.049	17.8	0.044	0.103
2	Bocq, Warche, Hoyoux, Salm	Mean	164.4	0.395	46.1	0.478	−0.011
		StD	60.98	0.138	33.5	0.042	0.030
3	Hermeton, Molignée, Vierre	Mean	40.00	0.358	15.2	0.360	0.239
		StD	26.46	0.037	3.1	0.091	0.146

Fig. 3. (A) Relation between the absolute height of the knickpoint and the mean uplift (MU). **(B)** Relation between the stream concavity index and (SCI) and the mean uplift (MU). The dotted line represents the expected relationship between the two indices **(C)** Relation between the local relief (LRel) and the mean uplift (MU). **(D)** Illustration of the three cluster groups within the Slope-Area space. The black crosses represent the first cluster (Aisne, Wamme and Hoegne rivers), the black dots the second cluster (Bocq, Warche, Hoyoux and Salm rivers), and the grey dots represent the third cluster (Hermeton, Molignée and Vierre rivers).

We analysed then the three clusters in the slope-area diagram (Fig. 3d). The constant of the power function equations corresponds to the intercept of the regression equation when plotted in a log-log scale, and can be interpreted in terms of steepness of the watershed, k_s. The slope of the regression line, θ, can be interpreted in terms of concavity of the catchment. The second cluster (Bocq, Warche, Hoyoux and Salm, represented with black dots Fig. 3d) is characterized by a low concavity index ($\theta = 0.34$) opposed to concavities

of 0.45 and 0.43 of the 1st (Aisne, Wamme and Hoegne, grey dots) and 3rd cluster (Hermeton, Molignée and Vierre, black crosses) respectively. Cluster 2 also differs from the other clusters in its steepness value (k_{sn}). Actually, a river with high intercept can be interpreted as having a greater steepness of its longitudinal profile. We can see the three clusters that have been designed by the k-mean analysis in the Fig. 3d. The first group (Hermeton, Molignée, Vierre; grey circles) has a Normalized Steepness (intercept) lower than
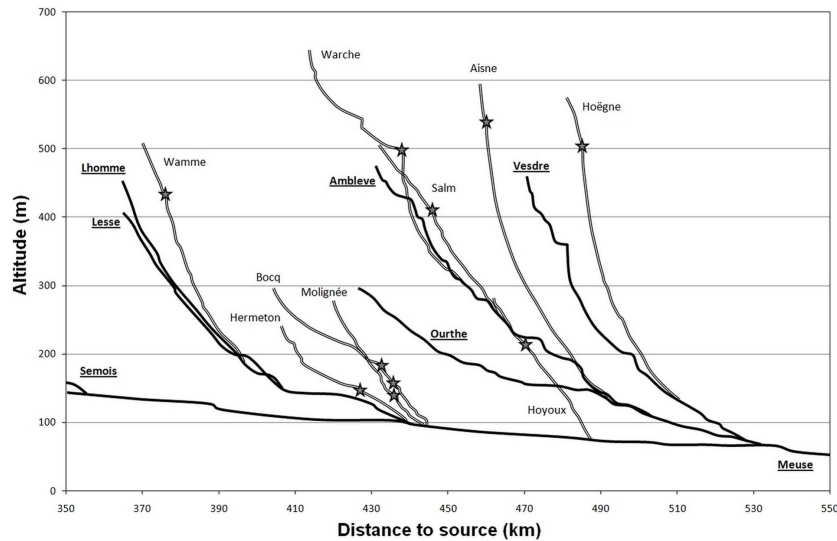
Fig. 4. Longitudinal profiles of the selected rivers within the Meuse river catchment. Double lines represent the selected rivers, bold lines the major streams of the region and stars indicate the position of the main knickpoint within each river profile. The Vierre profile is not represented in this graphic because of its distant location in the Semois river system.

the other groups. The second group is characterized by a relatively high value of steepness (Hoegne, Aisne, Wamme; black crosses). Finally, the last cluster of rivers (Warche, Bocq, Hoyoux, Salm; black dots) is considered as having a medium normalized steepness index, except for the Warche that has the highest steepness of the studied rivers. The fact that the Warche is in the same group than the Bocq, Hoyoux and Salm, is due to the fact that the clustering is multivariate and is also based on other river and hillslopes indexes (Rch, Ho, HI and SCI).

4   Discussion

In this paper, we used a selection of morphometric indexes that belong to different categories. Our analysis is based on channel related indexes (i.e. the river longitudinal profiles or the stream concavity index), catchment-wide indexes (i.e. Horton or the Hypsometric Integral), and also on indexes that are based on expert knowledge (i.e. the interpretation of geologic maps for the identification of knickpoints). Our results suggest that a single morphometric index cannot fully encompass the complex response of topography to tectonic uplift. A multivariate analysis of different slope and channel metrics that represent the complexity of multiple landscape components leads to a more accurate estimation of the exogenous agents that have shaped the landscape.

Our data on the river and channel morphology from a region with differential uplift rates indicate that the interaction between tectonic activity, slope and river processes is complex. The variability that we observe in slope morphology within the Ardennes Massif is not able to fully capture the complex response of the landscape to the tectonic im-
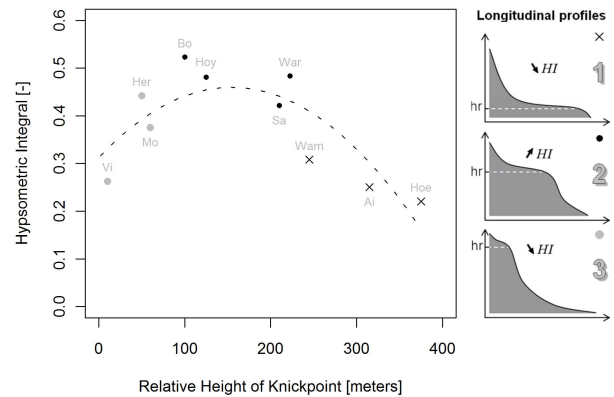

Fig. 5. Nonlinear relation between the relative height of the channel convexity (Rch) and the hypsometric integral (HI). Three phases of knickpoint upward migration are represented in the right panel.

print. The region of highest uplift is located in the northeastern part, and is characterized by high values of local relief (Fig. 3c) and steep river channels displaying clear convexities in the upper part of their river long profiles.

Despite the Quaternary uplift of the Ardennes Massif at low to moderate rates, the slope and channel morphology of third-order catchments is not yet in topographic steady-state, and exhibits clear convexities (or knickzones) in slope and river profiles (Fig. 1). Hence, the spatial variation that we observe in slope and channel morphology between the 10 third-order catchments is potentially not only the direct result of the differential uplift pattern, but might also reflect the transient adjustment of river channels to tectonic forcing.
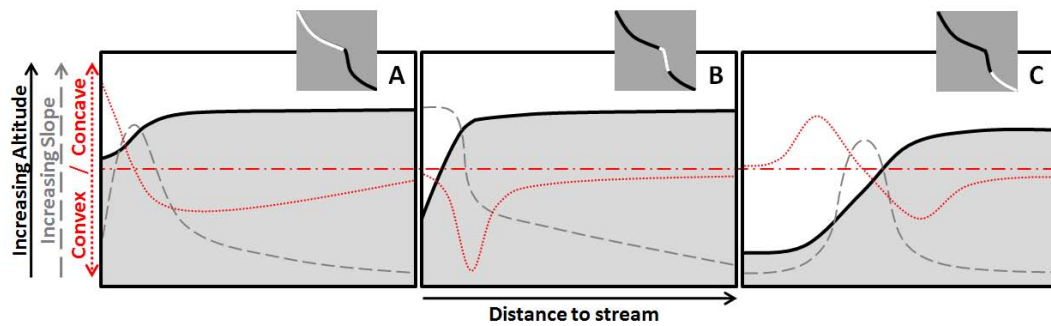
Fig. 6. Schematic representation of the change in hill slope morphology measured perpendicular to the river channel for three different positions: **(A)** upstream the river channel knick zone, **(B)** in the knick zone and **(C)** downstream the knick zone. The valley cross profiles are shown by the black line, the changes in stream proximal slopes by the dashed grey line and the stream proximal curvature by the red dotted line.

The Meuse River that is draining the third-order catchments acts as the local base level to which the fluvial system is adapting after the post 0.73 Ma tectonic uplift of the western Rhenish shield and the Ardennes (Fig. 1). Figure 4 clearly shows that the knick zones in the tributaries of the Meuse River are located at different heights, with the highest knick zones located in the northeastern part of the Ardennes Massif. This suggests that the response of the fluvial system was strongly diachronic, and that a transient signal of adjustment is migrating from the Meuse valley towards the Ardennian headwaters. This hypothesis is consistent with recent insights from ^{10}Be/^{26}Al dating of the Younger Main Terrace (YMT, frequently used geomorphic marker see Rixhon et al., 2011) of several Ardennian rivers. The absolute ages that Rixhon et al. (2011) obtain for the same terrace level within the Ardennes are significantly younger in the upstream parts of the lower Meuse valley, which suggests that the quaternary incision in the uplifted Ardennes Massif occurred diachronically. Rixhon et al. (2011) show that a $\sim$0.5 My timespan was needed by a tectonically induced incision wave to propagate from the lower Meuse towards the Ardennian headwaters, which contradicts the statement of a climatically driven incision that would have been synchronous throughout the Ardennes Massif.

Our data show some correlation between the overall river morphology and knickpoint migration. We broadly identified three types of catchments based on hypsometric and river channel analysis, and observed a nonlinear relation between the hypsometric integral, HI, and the relative position of the stream convexity, Rch (Fig. 5). Nevertheless, further analyses are needed to confirm the trends. Our data suggest that this relation underlines the K-mean grouping that has been presented in the previous section. The first morphological type (low HI, and low position of the convexity) broadly corresponds to river catchments with longitudinal profiles in equilibrium stage. Three catchments (Vierre, Hermeton, and Molignée) in the upper part of the Meuse catchment have such channel morphology, and seem not yet affected by the

base level changes following the uplift of the Ardennes Massif. The second type (high HI, medium relative height of convexity) contains catchments that were subject to recent tectonic activity (Bocq and Hoyoux) or that had higher tectonic uplift rates (Warche and Salm). The rivers that are draining regions with weaker lithologies or long incision history appear in the third group. This relation also indicates that the hypsometric integral alone is not adequate to determine the relative landform age or the adaptation stage of a river profile. Low values of the hypsometric integral may be present in catchments that are influenced by a tectonically-driven knickpoint (1st cluster), that have not yet been affected by knickpoint retreat and thus remained in equilibrium state (3rd cluster). This also highlights that a multivariate analysis, including HI, is necessary to fully understand the link between slope and channel morphology and tectonic activity.

When analysing the river transversal morphology, we can identify three morphological groups based on our observations of the slope and channel morphology of the selected catchments (indicated as A, B, C; in Fig. 6). The slope and channel morphology of these groups can be interpreted in terms of transient adjustment of the topography to relative base level change following uplift (Fig. 6). The first slope and channel morphology group (A) is typical for catchments that are located in the upper part of the catchments where a smooth channel-to-hillslope transition could be observed. This morphology was mostly observed for plateau regions, and corresponds to stream systems where slope and channel processes are coupled. The second and third group are transitional systems. The group B is characterized by very high and constant slopes close to the rivers and by a rapid transition to flat slopes. This scheme is typical for knick zones with a decoupling of channel and slope processes. The hillslopes surrounding a knickpoint area are often characterized by steep and straight slopes and are decoupled from the processes that affect the plateau area, which is located further upslope in the transversal profiles and characterized by a smooth sub-horizontal surface. The C scheme (smooth

S-curved slopes) can be seen as the later stage of evolution of the B scheme with the development of a large valley plain and with the highest slope gradients located at the middle part of the slopes. We found this C scheme often in the downstream part of the catchments, and it corresponds to recent rejuvenated topography. A similar study by Norton et al. (2008) characterized the basin morphometrics of a transient landscape in the forelands of the Swiss Alps, and indicated that the local hillslope curvature and slope angles can be used as a proxy to estimate the degree of rejuvenation in a catchment. Our study confirms the strength of stream proximal curvatures and stream proximal slopes as morphometric indices of relief adaptation following knickpoint retreat, but indicates that several forms of hillslope channel coupling can coexist within the same catchment based on the transient adjustment of the river channels to relative base level change.

5 Conclusions

Our data on slope and channel morphometric indexes from 10 catchments in the Ardennes massif suggest that river channel metrics are relevant indicators of the topographic signature of Quaternary uplift patterns in low relief landscapes. The morphometric analysis suggests that river channel morphology is a better indicator of geomorphic response to topographic uplift than the overall hillslope form and relief. The detailed picture for this region of low to moderate uplift rates is complex, but the data suggest some correlation between channel metrics and mean uplift rates while hillslope metrics appear to be rather insensitive to differential uplift. The combination of different morphometric indices in a multivariate cluster analysis reveals interesting results, but further morphometric analyses are needed to confirm the trends. Our study confirmed the strength of stream proximal curvatures and proximal slopes as indices of relief adjustment following knickpoint retreat.

We have indications that the river system is responding transiently to the low to moderate uplift rates observed for the Ardennes Massif. Significant longitudinal profile convexities are present, and the fluvial system seems to play an important role in the morphological adjustment to tectonic forcing. The spatial variation that we observe in slope and channel morphology between the 10 third-order catchments suggests that the response of the fluvial system was strongly diachronic, and that a transient signal of adjustment is migrating from the Meuse valley towards the Ardennian headwaters.

References

Ahnert, F.: Functional relationships between denudation, relief, and uplift in large, mid-latitude drainage basins, Am. J. Sci., 268, 243–263, 1970.

Bonnet, S. and Crave, A.: Landscape response to climate change: Insights from experimental modeling and implications for tectonic versus climatic uplift of topography, Geology, 31, 123–126, 2003.

Brocard, G. and van der Beek, P.: Influence of incision rate, rock strength and bedload supply on bedrock river gradients and valley-flat widths: Field-based evidence and calibrations from western Alpine rivers (SE France), Tectonics, Climate and Landscape Evolution, edited by: Willett, S. D., Hovius, N., Brandon, M. T., and Fisher, D.,, Geol. Soc. Am. Spec. Publ., 398, 101–126, 2006.

Burbank, D. and Anderson, R.: Tectonic Geomorphology, Wiley-Blackwell, 274 pp., 2000.

Burbank, D., Leland, J., Fielding, E., Anderson, R., Brozovic, N., Reid, M., and Duncan, C.: Bedrock incision, rock uplift and threshold hillslopes in the northwestern Himalayas, Nature, 379, 505–510, 1996.

Burbank, D., Blythe, A., Putkonen, J., Pratt-Sitaula, B., Gabet, E., Oskin, M., Barros, A., and Ojha, T.: Decoupling of erosion and precipitation in the Himalayas, Nature, 426, 652–655, 2003.

Camelbeeck, T., Alexander, P., Vanneste, K., and Meghraoui, M.: Long term seismicity in regions of present day low seismic activity: the example of western Europe, Soil Dyn. Earthqu. Eng, 20, 405–414, 2000.

Cloetingh, S., Ziegler, P., Beekman, F., Andriessen, P., Hardebol, N., and Dèzes, P.: Intraplate deformation and 3D rheological structure of the Rhine Rift System and adjacent areas of the northern Alpine foreland, Int. J. Earth Sci., 94, 758–778, 2005.

Demoulin, A.: L'Ardenne des Plateaux, héritage des temps anciens, surfaces d'érosion en Ardennes, in: L'Ardenne, essai de géographie physique, edited by: Demoulin, A., Dep. Géogr. Phys. Quat., Univ. Liège, 1995.

Demoulin, A.: Testing the tectonic significance of some parameters of longitudinal river profiles: the case of the Ardenne (Belgium, NW Europe), Geomorphology, 24, 189–208, 1998.

Demoulin, A. and Hallot, E.: Slope and amount of the Quaternary uplift of the western Rhenish shield and the Ardennes (western Europe), Tectonophysics, 474, 696–708, 2009.

Demoulin, A., Hallot, E. and Rixhon, G: Amount and controls of the Quaternary denudation in the Ardennes massif (western Europe), Earth Surface Processes and Landforms, 34, 1487–1496, 2009.

Douvinet, J., Delahaye, D., and Langlois, P.: Catchment morphgology and dynamics of hyper-concentrated stream flows on loamy plateaux (Basin Paris, in the North-Westren part of France), Sixth International Conference on Geomorphology (ICG), "Geomorphology in regions of environmental contrasts", 7–11 September, Zaragoza, Espagne, 2005.

Douvinet, J., Delahaye, D., and Langlois, P.: De la morphométrie à un champ de mesure de la structuration d'un bassin versant, Actes du Colloque International de Géomatique et d'Analyse Spatiale (SAGEO'2007), 18–20 June, Clermont-Ferrand, 2007.

Flint, J.: Stream gradient as a function of order, magnitude, and discharge, Water Resour. Res., 10, 969–973, 1974.

Garcia-Castellanos, D., Cloetingh, S., and van Balen, R.: Modelling the Middle Pleistocene uplift in the Ardennes-Rhenish Massif:

thermo-mechanical weakening under the Eifel?, Global Planet. Change, 27, 39–52, 2000.

Grimaldi, S., Nardi, F., Di Benedetto, F., Istanbulluoglu, E., Bras, R. L.: A physically based method for removing pits in digital elevation models, Adv. Water Res., 30, 2151–2158, 2007.

Grimbérieux, J., Laurant, A., and Ozer, P.: Les rivières s'installent, in: L'Ardenne. Essai de géographie physique, Hommage au professeur Pissart, A., edited by: Demoulin, A., Département de géographie physique et du Quaternaire, Université de Liège, 1995.

Grohmann, C. and Riccomini, C.: Comparison of roving-window and search-window techniques for characterising landscape morphometry, Comput. Geosci., 35, 2164–2169, 2009.

Hack, J.: Stream-profile analysis and stream-gradient index, US Geological Survey Journal of Research, 1, 421–429, 1973.

Horton, H.: Drainage basin characteristics, Trans. Amer. Geophys. Union, 13, 350–361, 1932.

Horton, H.: Erosional development of streams and their drainage basins, Geological Society of America, 56, 275–370, 1945.

Howard, A., Dietrich, W., and Seidl, M.: Modeling fluvial erosion on regional to continental scales, J. Geophys. Res., 99, 13971–13986, 1994.

IGN: Website of the National Geographical Institute of Belgium: last visit on 13 April 2008, available at: www.ngi.be, 2008a.

IGN: DTM 1:10 000 Wallonie, Technical report provided by the National Geographical Institute of Belgium, last update 14 May 2008, 2008b.

Inoue, K.: Downstream change in grain size of river bed sediments and its geomorphological implications in the Kanto Plain, central Japan, Geographical Review of Japan, 65, 75–89, 1992.

Juvigné, E. and Renard, F.: Les terraces de la Meuse, de Liege à Maastricht, Annales de la société géologique de Belgique, 115, 167–186, 1992.

Kamp, U., Bolch, T., and Olsenholler, J.: Geomorphometry of Cerro Sillajhuay, Chile/Bolivia: comparison of DEMs derived from ASTER remote sensing data and contour maps, Geocarto International, 20, 23–34, 2005.

Kirby, E. and Whipple, K.: Quantifying differential rock-uplift rates via stream profile analysis, Geology, 29, 415–418, 2001.

Kirby, E., Whipple, K., Burchfiel, B., Tang, W., Berger, G., Sun, Z., and Chen, Z.: Neotectonics of the Min Shan, China: Implications for mechanisms driving Quaternary deformation along the eastern margin of the Tibetan Plateau, Geol. Soc. Am. Bull., 112, 375–393, 2000.

Lague, D. and Davy, P.: Constraints on the long-term colluvial erosion law by analyzing slope-area relationships at various tectonic uplift rates in the Siwaliks Hills (Nepal), J. Geophys. Res., 108, 2129, doi:10.1029/2002JB001893, 2003.

Lague, D., Davy, P., and Crave, A.: Estimating uplift rate and erodibility from the area-slope relationship: Examples from Brittany (France) and numerical modelling, Phys. Chem. Earth, 25, 543–548, 2000.

Luo, W.: Hypsometric analysis with a Geographic Information System, Compu. Geosci., 24, 815–821, 1998.

Lu, Y., Lu, S., Fotouhi, F., Deng, Y., and Brown, S.: FGKA: A Fast Genetic K-means Algorithm, in Proc. of the 19th ACM Symposium on Applied Computing, 162–163, Nicosia, Cyprus, 2004.

Maddy, D.: Uplift-driven valley incision and river terrace formation in southern England, J. Quaternary Sci., 12, 539–545, 1997.

Meyer, W. and Stets, J.: Junge Tektonik im Rheinischen Schiefergebirge und ihre Quantifizierung, Zeitschrift der Deutschen Geologischen Gesellschaft, 149, 359–379, 1998.

Montgomery, D. and Brandon, M.: Topographic controls on erosion rates in tectonically active mountain ranges, Earth Planet. Sci. Lett., 201, 481–489, 2002.

Musumeci, G. and Colombo, F.: Late Visean mylonitic granitoids in the Argentera Massif (Western Alps): age and kinematic constraints on the Fèrriere Mollière shear zone, Comptes Rendus de l'Academie des Sciences Serie II Fascicule A-Sciences, 334, 213–220, 2002.

Nardi, F., Grimaldi, S., Santini, M., Petroselli, A., and Ubertini, L.: Hydrogeomorphic properties of simulated drainage patterns using digital elevation models: the flat area issue, Hydrol. Sci. J., 53(6), 1176–1193, 2008.

Norton, K., von Blanckenburg, F., Schlunegger, F., Schwab, M., and Kubik, P.: Cosmogenic nuclide-based investigation of spatial erosion and hillslope channel coupling in the transient foreland of the Swiss Alps, Geomorphology, 95, 474–486, 2008.

Petit, F., Gob, F., Houbrechts, G., and Assani, A.: Critical specific stream power in gravel-bed rivers, Geomorphology, 69, 92–101, 2005.

Pissart, A.: La Meuse en France et en Belgique. Formation du basin hydrographique. Les terraces et leurs enseignements, In: Macar, P. (Ed.), Centenaire de la Soc. Géol. De Belg. L'évolution quaternaire des basins fluviaux de la mer du Nord méridionale, Liège, Belgium, 105–131, 1974.

Pissart, A. and Lambot, P.: Les mouvements actuels du sol en Belgique; comparaison de deux nivellements IGN (1946–1948 et 1976–1980), Ann. Soc. Géol. Belg., 112, 495–504, 1989.

Pissart, A., Harmand, D., and Krook, L.: L'évolution de la Meuse de Toul à Maastricht depuis le Miocène. Corrélations chronologiques et traces des captures de la Meuse lorraine d'après les minéraux denses, Géographie Physique et Quaternaire, 51, 267–284, 1997.

Rice, S. and Church, M., Grain size along two gravel-bed rivers: statistical variation, spatial pattern and sedimentary links, Earth Surface Processes and Landforms, 23, 345–363, 1998.

Ritter, J., Jordan M., Christensen, U., and Achauer, U.: A mantle plume below the Eifel volcanic fields, Germany, Earth Planet. Sci. Lett., 186, 7–14, 2001.

Rixhon, G., Braucher, R., Bourlès, D., Siame, L., Bovy, B., and Demoulin, A.: The quaternary river incision in the NE Ardennes (Belgium) – insights from 10Be/26Al dating of river terraces, Quaternary Geochronology, 6, 273–284, 2011.

Roe, G., Montgomery, D., and Hallet, B.: Effects of orographic precipitation variations on the concavity of steady-state river profiles, Geology, 30, 143–146, 2002.

Santini, M., Grimaldi, S., Nardi, F., Petroselli, A., and Rulli, M. C.: Preprocessing algorithms and landslide modelling on remotely sensed DEMs, Geomorphology, 113, 110–125, 2009.

Senadeera, K., Piyasiri, S., and Nandalal, K.: The evaluation of Morphmetric Characteristics of Kotmale Reservoir catchment using GIS as a tool, Sri Lanka, The International Archives of the Photogrammetry, Remote Sens. Spatial Information Sciences, 34, Part XXX, 2004.

Schaller, M., von Blanckenburg, F., Hovius, N., Veldkamp, A., Van den Berg, M., and Kubik, P.: Paleoerosion rates from cosmogenic 10Be in a 1.3 Ma terrace sequence: response of the River Meuse

Hydrol. Earth Syst. Sci., 15, 1095–1107, 2011

www.hydrol-earth-syst-sci.net/15/1095/2011/

to changes in climate and rock uplift, J. Geol., 112, 127–144, 2004.

Schäuble, H.: Erosionsmodellierungen mit GIS. Probleme und Lösungen zur exakten Prognose von Erosion und Akkumulation, in: Ergebnisse der Jahrestagung des Arbeitskreises GIS 25/26, Tübingen, 51–62, 2000.

Schneider, H., Schwab, M., and Schlunegger, F.: Channelized and hillslope sediment transport and the geomorphology of mountain belts, Int. J. Earth Sci., 97, 179–192, 2008.

Snyder, N., Whipple, K., Tucker, G., and Merritts, D.: Landscape response to tectonic forcing: DEM analysis of stream profiles in the Mendocino Triple junction region, Northern California, Geological Society of America Bulletin, 112, 1250–1263, 2000.

Snyder, N., Whipple, K., Tucker, G., and Merritts, D.: Channel response to tectonic forcing: field analysis of stream morphology and hydrology in the Mendocino triple junction region, northern California, Geomorphology, 53, 97–127, 2003.

Strahler, A.: Hypsometric (area-altitude) analysis of erosional topology, Geological Society of America Bulletin, 63, 1117–1142, 1952.

Surian, N.: Downstream variation in grain size along an Alpine river: analysis of controls and processes, Geomorphology, 43, 137–149, 2002.

Tarboton, D., Bras, R., and Rodriguez-Iturbe, I.: On the Extraction of Channel Networks from Digital Elevation Data, Hydrol. Process., 5, 81–100, 1991.

Tebbens, L., Veldkamp, A., Van Dijke, J., and Schoorl, J.: Modeling longitudinal-profile development in response to Late Quaternary tectonics, climate and sea-level changes: the River Meuse, Global Planet. Change, 27, 165–186, 2000.

Tesauro, M., Kaban, M., and Cloetingh, S.: A new thermal and rheological model of the European lithosphere, Tectonophysics, 476, 478–495, 2009.

Tibaldi, A. and Leon, J.: Morphometry of late Pleistocene–Holocene faulting and volcanotectonic relationship in the southern Andes of Colombia, Tectonics, 19, 358–377, 2000.

Törnqvist, T.: Longitudinal profile evolution of the Rhine–Meuse system during the last deglaciation: interplay of climate change and glacio-eustasy?, Terra Nova, 10, 11–15, 1998.

Van Balen, R., Houtgast, R., Van der Wateren, F., Vandenberghe, J., and Bogaart, P.: Sediment budget and tectonic evolution of the Meuse catchment in the Ardennes and the Roer Valley Rift System, Global Planet. Change, 27, 113–129, 2000.

Vanacker, V., von Blanckenburg, F., Govers, G., and Kubik, P.: Transient landscape evolution following uplift in the Southern Ecuadorian Andes, Geochim. Cosmochim. Acta, 71, A1052, 2007.

Van den Berg, M.: Fluvial sequences of the Maas, a 10Ma record of neotectonics and climate change at various time-scales, Wageningen, 181 pp., 1996.

Vandycke, S.: Palaeostress records in Cretaceous formations in NW Europe: extensional and strike-slip events in relationships with Cretaceous-Tertiary inversion tectonics, Tectonophysics, 357, 119–136, 2002.

Veldkamp, A. and van den Berg, M.: Three-dimensional modeling of Quaternary fluvial dynamics in a climo-tectonic dependent system. A case study of the Maas record (Maastricht, the Netherlands), Global Planet. Change, 8, 203–218, 1993.

Wang, L. and Liu, H.: An efficient method for identifying and filling surface depressions in digital elevation models for hydrologic analysis and modelling, International Journal of Geographical Information Science, 20, 193–213, 2006.

Weissel, J., Pratson, L., and Malinverno, A.: The length-scaling properties of topography, J. Geophys. Res., 99, 13997–14012, 1994.

Whipple, K.: Bedrock rivers and the geomorphology of active orogens, Annu. Rev. Earth Planet. Sci., 32, 151–185, 2004.

Whipple, K., Kirby, E., and Brocklehurst, S.: Geomorphic limits to climate-induced increases in topographic relief, Nature, 401, 39–43, 1999.

Whipple, K. and Tucker, G.: Dynamics of the Stream Power River Incision Model: Implications for Height Limits of Mountain Ranges, Landscape Response Timescales and Research Needs, J. Geophys. Res., 104, 17661–17674, 1999.

Whipple, K. and Tucker, G.: Implications of sediment-flux-dependent river incision models for landscape evolution, J. Geophys. Res., 107(B2), 2039, doi:10.1029/2000JB000044, 2002.

Willgoose, G. and Hancock, G.: Revisiting the hypsometric curve as an indicator of form and process in transport-limited catchment, Earth Surface Processes and Landforms, 23, 611–623, 1998.

Wobus, C., Hodges, K., and Whipple, K.: Has focused denudation sustained active thrusting at the Himalayan topographic front, Geology, 31, 861–864, 2003.

Zaprowski, B., Pazzaglia, F., and Evenson, E.: Climatic influences on profile concavity and river incision, J. Geophys. Res., 110, F03004, doi:10.1029/2004JF000138, 2005.